AIAA JOURNAL
Vol. 36, No. 6, June 1998

Modeling the Flow of Water on Aircraft in Icing Conditions

Tim G. Myers* and Chris P. Thompson†
Cranfield University, Cranfield, Bedfordshire, England MK 43 0AL, United Kingdom

A three-dimensional mathematical model that describes the flow of a thin film of water driven by air shear, gravity, surface tension, and ambient pressure variation over a solid substrate is derived. The one-dimensional version is then analyzed and numerical solutions for the fluid film height and velocity obtained. After further simplifying assumptions, a number of formulas that relate film heights and average velocities to the strength of the air shear or gravity effects are also presented.

I. Introduction

A FUNDAMENTAL problem in the aerospace industry concerns the buildup of ice on lifting surfaces and surfaces where ice may break off and subsequently damage other components.[1] To combat this problem, aircraft are sprayed with anti-icing fluid while on the ground to prevent ice from forming on critical surfaces. During flight in icing conditions, one option is to heat vulnerable surfaces. This may require a considerable amount of energy. For example, the power required by a typical electrothermal ice protection system on a helicopter can account for over 10% of the engine power. Also, the trend toward the use of higher-bypass-ratio turbofan engines in the fixed-wing-aircraft industry consequently means that the amount of available core engine bleed air for anti-icing purposes is becoming smaller. Hence, as well as the obvious safety aspects, there are compelling financial reasons for investigating this phenomenon.

Ice will typically form when supercooled water droplets, from clouds, mist, or freezing drizzle, hit an aircraft and subsequently freeze. Depending on the atmospheric and flight conditions, the ice that forms on the aircraft will be either rime ice, glaze ice, or a mixture of the two. With glaze ice, the droplets that impinge on the surface do not freeze instantaneously but form a film of liquid water that runs back over the surface, freezing gradually at various rates. In current icing codes, all of this unfrozen water is dealt with by moving it to an adjacent computational cell at the next time step (see, for example, Ref. 2). In reality the water motion will depend on the driving forces, and only a portion of it will occupy the next cell. Because the behavior of the water film will have a significant effect on the shape of the resulting ice formation, there is a need for a detailed study into the flow of a thin layer of water on a solid surface as part of an investigation into the formation of glaze ice (see, for example, Refs. 3 and 4).

Experiments carried out under typical glaze ice conditions reveal three distinct zones of ice formation.[3] The first, in the vicinity of the stagnation point, is composed of an ice surface with no distinct roughness. On top of the ice is a thin continuous film of water. Somewhere behind this region lies a rough zone where water typically beads. If ice is allowed to build up over a sufficient time, this rough zone may envelop the smooth one. Behind this is the runback zone. The work in this paper is clearly applicable to the central region, which is largest at early times in the development of ice. Moreover, experiments on the growth of ice in the rough zone will produce different small-scale features each time, but large-scale features are usually reproducible. To numerically predict the large-scale features is the best that can be expected from an icing code. To achieve this, an average flow needs defining, rather than modeling individual water beads that may shelter behind ice crystals or even fluid that may experience a higher shear through air funneling effects. For this reason the model will be applicable in the rough zone as well.

The method and results described in the following sections have a number of practical uses other than modeling glaze ice growth. For example, fluid flow driven by interfacial shear, gravity, and surface tension is important in the study of compact heat exchangers, trickle bed reactors, spray coating, and blow drying (see, for example, Refs. 5 and 6). An aircraft component, heated to prevent ice accretion, may be covered at the leading edge by a continuous liquid film, provided the collection efficiency is sufficiently high. The whole question of atmospheric ice accretion is also of interest to marine engineers and power companies whose overhead transmission lines are prone to icing.[7]

Previous analytical studies of fluid flow on aircraft have largely neglected the effect of surface tension. However, its inclusion is clearly justified by the experiments reported in Refs. 3 and 8 in which results show dramatic changes in ice shapes with varying surface tension.

The theory developed in this paper will ultimately be incorporated into a three-dimensional aircraft icing code, ICECREMO. Because it is envisaged, in the preliminary version at least, to use spline segments to discretize the aircraft surface, only flow in a Cartesian coordinate system will be considered. For this reason, a fully three-dimensional mathematical model is developed in the following section. However, only the simpler one-dimensional model is analyzed in detail, to determine simplified relationships between the driving forces and the film height.

Flow stability will not be considered in the present work. Although the interactions between the airflow and surface waves, hole, and rivulet formation are important effects, the present solution should be seen as a leading order one, where perturbations to the base state are neglected. More information on these stability modes may be found in Refs. 9–13.

II. Mathematical Theory

A. Three-Dimensional Flow Description

In this initial study only isothermal flow will be considered; hence freezing and evaporation are neglected, as is the effect of incoming droplets.

Fluid is assumed to be flowing down an inclined plane, at an angle α to the horizontal, under the influence of gravity, interfacial shear, and surface tension. The film has thickness h; the coordinates are such that x is directed down the plane and z is perpendicular to the plane. The Navier–Stokes equations are assumed to govern the fluid flow; however, to model the thin liquid film, these may be reduced using lubrication theory (see, for example, Ref. 14). The basis of this is that changes across the film must happen over a much shorter length scale than those along the film. With an appropriate scaling the dominant terms may then be picked out, giving

$$\frac{\partial p}{\partial z} \approx -\rho g \hat{\boldsymbol{g}} \cdot \hat{\boldsymbol{z}} \tag{1}$$

Received April 9, 1997; revision received Aug. 23, 1997; accepted for publication Jan. 19, 1998.

*Research Officer, Applied Mathematics and Computing Group. E-mail: t.g.myers@cranfield.ac.uk.

†Senior Lecturer, Applied Mathematics and Computing Group.

$$\mu \frac{\partial^2 u}{\partial z^2} \approx \frac{\partial p}{\partial x} - \rho g \hat{\boldsymbol{g}} \cdot \hat{\boldsymbol{x}} \tag{2}$$

$$\mu \frac{\partial^2 v}{\partial z^2} \approx \frac{\partial p}{\partial y} - \rho g \hat{\boldsymbol{g}} \cdot \hat{\boldsymbol{y}} \tag{3}$$

where p is the fluid pressure, (u, v, w) is the velocity vector, and μ and ρ are the fluid viscosity and density, respectively. For an incompressible fluid the continuity equation is unaffected by lubrication theory:

$$\frac{\partial u}{\partial x} + \frac{\partial v}{\partial y} + \frac{\partial w}{\partial z} = 0 \tag{4}$$

Equations (1–3) demonstrate that the main driving forces within the fluid are gravity and pressure gradients.

The appropriate boundary conditions for solving this system are as follows: On the solid surface there is no slip, while on the free surface the normal stress is balanced by surface tension, shear stress is continuous, and the kinematic condition holds. Mathematically these imply

$$u = v = w = 0 \tag{5}$$

on the substrate, $z = f(x, y)$. On the free surface, $z = h(x, y)$:

$$p - p_a = -\sigma \nabla^2 h \tag{6}$$

$$\mu \frac{\partial u}{\partial z} = T_1, \qquad \mu \frac{\partial v}{\partial z} = T_2 \tag{7}$$

$$w = \frac{\partial h}{\partial t} + u \frac{\partial h}{\partial x} + v \frac{\partial h}{\partial y} \tag{8}$$

where p_a is the ambient pressure (which may vary over the fluid surface), σ is the surface tension, (T_1, T_2) is the shear stress caused by the airflow, and h is the film height. Note that the solid surface is not necessarily flat; the function $f(x, y)$ may model surface roughness or curvature and must be input to the calculation. Setting $f \equiv 0$ reduces the problem to flow down a flat substrate.

Subject to these conditions, Eqs. (1–3) may now be integrated to give

$$p - p_a = -\rho g \hat{\boldsymbol{g}} \cdot \hat{\boldsymbol{z}} (z - h) - \sigma \nabla^2 h \tag{9}$$

$$\mu u = \frac{1}{2}\left(\frac{\partial p}{\partial x} - \rho g \hat{\boldsymbol{g}} \cdot \hat{\boldsymbol{x}}\right)[(z^2 - f^2) - 2h(z - f)] + T_1(z - f) \tag{10}$$

$$\mu v = \frac{1}{2}\left(\frac{\partial p}{\partial y} - \rho g \hat{\boldsymbol{g}} \cdot \hat{\boldsymbol{y}}\right)[(z^2 - f^2) - 2h(z - f)] + T_2(z - f) \tag{11}$$

These expressions show that the pressure varies linearly with z, whereas velocities vary with z^2. All of these quantities depend on the unknown position of the free surface h.

The film height may be determined by substituting Eqs. (10) and (11) into Eq. (4), integrating over the film, and applying the kinematic condition (8) to eliminate the velocity in the z direction. This leads to the single equation

$$\mu \frac{\partial (h - f)}{\partial t} + \nabla \cdot \left[\frac{(h - f)^3}{3}\left(\sigma \nabla \nabla^2 h - \rho g \hat{\boldsymbol{g}} \cdot \hat{\boldsymbol{z}} \nabla h + \rho g (\hat{\boldsymbol{g}} \cdot \hat{\boldsymbol{x}}, \hat{\boldsymbol{g}} \cdot \hat{\boldsymbol{y}}) - \nabla p_a\right) + \frac{(h - f)^2}{2} \boldsymbol{T}\right] = 0 \tag{12}$$

This is a fourth-order nonlinear partial differential equation. It shows that, in the absence of freezing and/or evaporation, the film thickness varies due to surface tension, gravity, air shear, substrate shape, and ambient pressure variation. Once it is solved, fluid velocities and pressure throughout the film may be calculated.

Note that the surface tension term and the first gravity term of Eq. (12) stabilize the film (provided the coupling with the airflow is neglected); that is, they effectively act as a damping force. This may easily be shown mathematically for small perturbations to the equilibrium state (see, for example, Ref. 15). Hence, given a sufficiently long region, the film may be expected to reach an equilibrium height. This will be exploited in solving the numerical scheme of the following section. Any interaction with the airflow would be reflected in the ∇p_a term. A further equation would also be required to describe the airflow. This problem is considered in Ref. 13.

B. Two-Dimensional Steady-State Analysis

Equation (12) models three-dimensional unsteady flow on a substrate and can be incorporated into a full numerical scheme. However, to simplify the analysis and to gain a better physical understanding of the process, a number of further assumptions can be made. First, although the air pressure may vary considerably near the leading edge of an airfoil, in general the ambient pressure will remain approximately constant; ∇p_a will thus be set to zero. For a fluid film, or over the central region of a rivulet, the flow will be basically unidirectional and so a two-dimensional model will be considered. Finally, the flow will be assumed to have reached a steady state, and so $\partial h/\partial t = 0$. Equation (12) may then be integrated to

$$\frac{h^3}{3}\left(\sigma \frac{\partial^3 h}{\partial x^3} - \rho g \frac{\partial h}{\partial x} \cos\alpha + \rho g \sin\alpha\right) + \frac{h^2}{2} T_1 = \mu Q \tag{13}$$

where Q is the fluid flux per unit length in the y direction.

Equation (13) may be readily solved numerically, once appropriate boundary conditions are prescribed. For the present study it will be assumed that the film height at $x = 0$ is known (in the icing computational fluid dynamics code this will be determined using data from the previous cell) and that the cell of interest is sufficiently long for the fluid to attain its equilibrium height before the end is reached. Equivalently, this would model a flow where fluid is pumped at a constant rate from an inlet of known height onto a sloping plane.

The actual solution method employed was to determine the limiting value of Eq. (13), from Eq. (14), and to perturb this to give values of h, h_x, and h_{xx}, which are required as the starting point for an initial value solver. The solution is then marched, using a fourth-order Runge–Kutta algorithm, up to the specified inlet height and the calculation ended. Typical film heights were calculated for varying values of the air shear, $T_1 = 0$, 1, and 10 N/m^2, with a slope of 45 deg and a fluid flux per unit length in the y direction of 10^{-4} m^2/s. These are shown as curved lines on Fig. 1, where the uppermost curve corresponds to $T_1 = 0$ and the lowest to $T_1 = 10$ (equivalent to air speeds on the order of 0 and 1000 kph, respectively).

Mainly due to the effect of surface tension, the fluid film height rapidly adjusts, near the inlet, from its initial height to its equilibrium value. For zero air shear the fluid requires approximately 0.6 cm to attain its equilibrium height. Increasing the air shear forces the film to reach its equilibrium height more rapidly; when $T_1 = 10$ it only takes 0.3 cm. It also causes a significant decrease in the final thickness.

Because the terms involving derivatives of h act to bring the film toward its equilibrium height, far enough away from the inlet these terms will be negligible. Hence, a simple formula may be obtained for the equilibrium height, which is the real root of

$$2\rho g \sin\alpha h^3 + 3T_1 h^2 = 6\mu Q \tag{14}$$

Even simpler relations may be obtained for the limiting cases of large and small air shear, h_s and h_g; these are

$$h_s = \sqrt{\frac{2\mu Q}{T_1}}, \qquad h_g = \left(\frac{3\mu Q}{\rho g \sin\alpha}\right)^{\frac{1}{3}} \tag{15}$$

These expressions will be valid away from the inlet when T_1 is large or small in comparison with $2\rho g \sin\alpha h/3$ ($\approx 6.5 \times 10^3 h \sin\alpha$). They are also plotted on Fig. 1; h_s is shown as the lowest straight line, which matches the equilibrium height from the numerical result for $T_1 = 10$ to within 3%; h_g is shown as the upper straight line, which, as expected, coincides almost exactly with the numerical result for $T_1 = 0$. The simplest results, calculated from Eq. (15), have subsequently been found to agree within 20% of a finite element

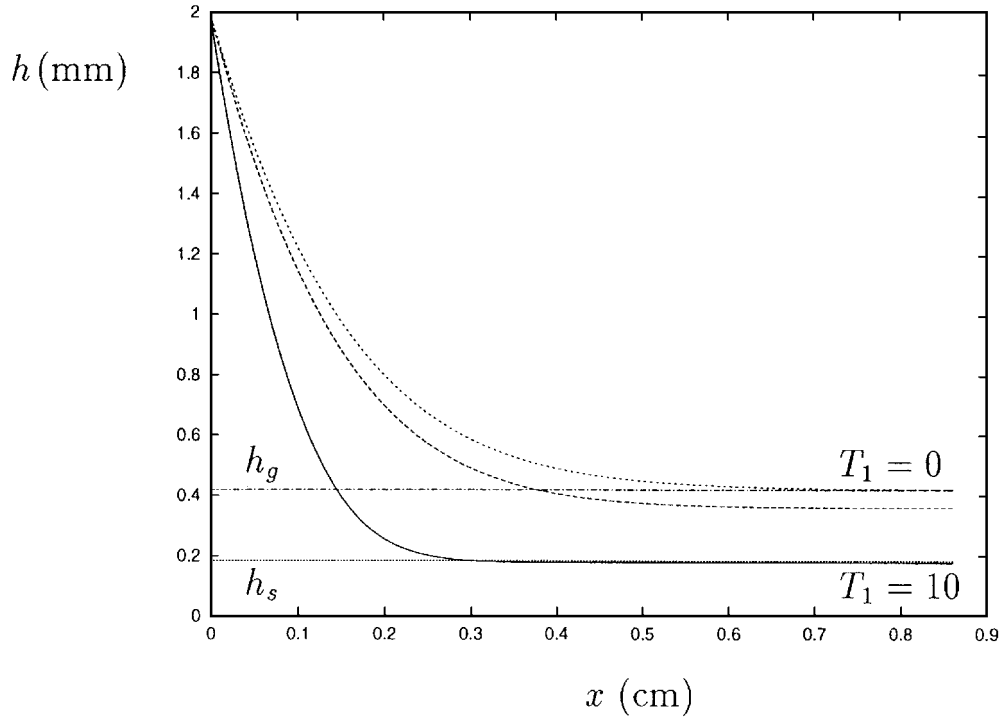

Fig. 1 Film shape for varying air shear with T_1 = 0, 1, and 10 N/m^2 and limiting values for zero and large air shear.

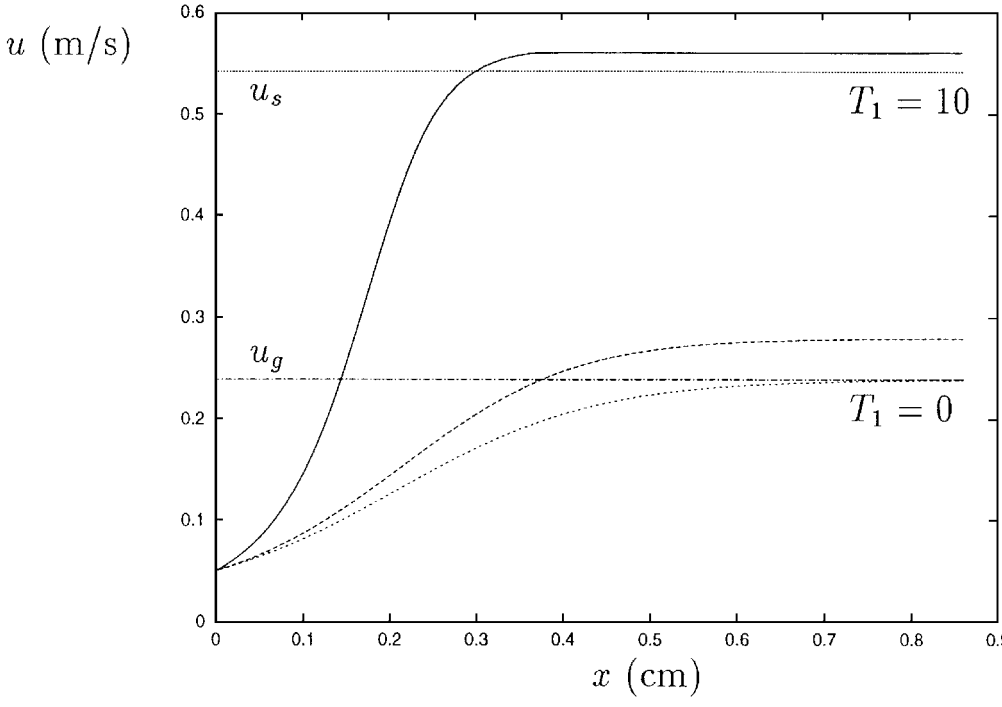

Fig. 2 Average velocity for varying air shear with T_1 = 0, 1, and 10 N/m^2 and limiting values for zero and large air shear.

calculation.[16] The source of the discrepancy most likely comes from numerical errors rather than the analytical formulas.

The average velocity through the film is given by

$$\bar{u} = \frac{1}{h}\int_0^h u\,\mathrm{d}z \tag{16}$$

$$= \frac{h^2}{3\mu}\left[\sigma\frac{\partial^3 h}{\partial x^3} - \rho g\left(\frac{\partial h}{\partial x}\cos\alpha - \sin\alpha\right)\right] + \frac{T_1 h}{2} \tag{17}$$

In Fig. 2 average velocities, corresponding to the examples of Fig. 1, are plotted. Now the highest curve corresponds to the highest value of air shear and the lowest to zero air shear. Near the inlet, where the film height is greatest, the average velocity is low, but as the film thickness decreases, the velocity increases and rapidly reaches its equilibrium value. As expected, both from the physical point of view as well as from continuity arguments, the higher the air shear the higher the equilibrium velocity.

Substituting the film height obtained from Eq. (14) into Eq. (17) will lead to a general expression for the average velocity away from the inlet. The limiting cases for large and small air shear may be obtained as

$$\bar{u}_s = \sqrt{\frac{QT_1}{2\mu}}, \qquad \bar{u}_g = \left(\frac{Q^2\rho g\sin\alpha}{3\mu}\right)^{\frac{1}{3}} \tag{18}$$

These are also shown as straight lines on Fig. 2; again the zero air shear result coincides with the $T_1 = 0$ curve, whereas for high air shear the result differs by 3%.

III. Conclusion

The main objectives of this work were to develop a model equation for the flow of a water layer, which could be incorporated into an icing code, and to develop a number of simple results to test its validity. The mathematical model was derived in Sec. II. The steady-state, two-dimensional version of this equation for film height was then considered. Numerical solutions show that surface tension quickly acts to level the fluid film to its equilibrium height, which is determined by the fluid flux and the relative strength of the air shear to gravity forces. As may be expected from physical observations, the film thickness decreases with increasing air shear, whereas the average velocity increases due to the increase in drag.

A number of simple relations were also obtained, giving the equilibrium film height for the limiting cases of large and small air shear. The limiting cases showed the film height varying with the inverse square root of the magnitude of the air shear or the inverse cube root of gravity. The corresponding velocities vary with the square root of air shear and the cube root of gravity. A comparison of the limiting formulas with the numerical results showed excellent agreement; the discrepancy of 3% obtained for the high air shear case will further decrease as T increases.

Because of the assumptions made in deriving the present model, the results should not be expected to accurately describe all types of thin film flow driven by air shear. In particular, although the model equation (12) is time dependent, the results presented are for steady-state flow; future work will include nonsteady effects. The ambient pressure variation has been neglected, and although this may be reasonable in many situations, it is clearly not the case near the leading edge of an airfoil. However, there is a term in the governing equation (12) that allows for pressure variation and could be input from an external computational fluid dynamics calculation. Alternatively, by choosing a sufficiently small domain, the ambient pressure variation could be made relatively small. A number of other effects could easily be incorporated into the model; at the moment the authors are investigating rotating systems, where centrifugal forces play an important role, and also rivulet flow; surface roughness effects, the impingement of water from a cloud, and freezing are also important. Finally, there are a number of stability questions that have not been addressed here, such as hole formation, film breakup into rivulets, and the interaction between the air and liquid flow that can speed up the fluid and lead to wave development.

Acknowledgments

The ICECREMO project (the development of three-dimensional ice accretion modeling) is a collaboration between British Aerospace, Rolls–Royce, Westland Helicopters, and the Defence Evaluation and Research Agency. The project is managed by British Aerospace and is partly funded by the Department of Trade and Industry under Contract RA/6/31/05.

References

[1]Thomas, S. K., Cassoni, R. P., and MacArthur, C. D., "Aircraft Anti-Icing and De-Icing Techniques and Modeling," *Journal of Aircraft*, Vol. 33, No. 5, 1996, pp. 841–854.

[2]Cansdale, J. T., "Helicopter Rotor Ice Accretion and Protection Research," *Vertica*, Vol. 5, No. 4, 1981 pp. 357–368.

[3]Hansman, R. J., Jr., and Turnock, S. R., "Investigation of Surface Water Behavior During Glaze Ice Accretion," *Journal of Aircraft*, Vol. 26, No. 2, 1989, pp. 140–147.

[4]Al-Khalil, K. M., Keith, T. G., Jr., and De Witt, K. J., "New Concept in Runback Water Modeling for Anti-Iced Aircraft Surfaces," *Journal of Aircraft*, Vol. 30, No. 1, 1993, pp. 41–49.

[5]Moriarty, J. A., Schwartz, L. W., and Tuck, E. O., "Unsteady Spreading of Thin Liquid Films with Small Surface Tension," *Physics of Fluids*, Vol. A3, No. 5, 1991, pp. 733–742.

[6]Paul, S., *Surface Coatings: Science and Technology*, Wiley-Interscience, New York, 1985, Chap. 1.

[7]Poots, G., *Ice and Snow Accretion on Structures*, Research Studies Press, Somerset, England, UK, 1996, Chap. 1.

[8]Bilanin, A. J., and Anderson, D. N., "Ice Accretion with Varying Surface Tension," AIAA Paper 95-0538, Jan. 1995.

[9]Bertozzi, A. L., Brenner, M. P., Dupont, T. F., and Kadanoff, L. P., "Singularities and Similarities in Interface Flows," *Trends and Perspectives in Applied Mathematics*, Vol. 100, Applied Mathematical Science, Springer–Verlag, Berlin, 1993, pp. 155–208.

[10]Hanratty, T. J., "Interfacial Instabilities Caused by Air Flow over a Thin Liquid Layer," *Waves on Fluid Interfaces*, edited by R. E. Meyer, Academic, London, 1983, pp. 221–259.

[11]Schwartz, L. W., "Viscous Flows Down an Inclined Plane: Instability and Finger Formation," *Physics of Fluids*, Vol. A1, No. 3, 1989, pp. 443–445.

[12]Silvi, N., and Dussan, V. E. B., "On the Rewetting of an Inclined Solid Surface by a Liquid," *Physics of Fluids*, Vol. 28, No. 1, 1985, pp. 5–7.

[13]Tsao, J.-C., Rothmayer, A. P., and Ruban, A. I., "Stability of Air Flow Past Thin Liquid Films on Airfoils," *Computers and Fluids*, Vol. 26, No. 5, 1997, pp. 427–452.

[14]Cameron, A., *Basic Lubrication Theory*, 3rd ed., Ellis Horwood, Chichester, England, UK, 1981.

[15]Myers, T. G., "Surface Tension Driven Thin Film Flows," *SIAM Review* (to be published).

[16]Myers, T. G., Thompson, C. P., and Bandakhavai, V. K. S. S., "Modelling Water Flow on Aircraft in Icing Conditions. Part I: Theory and Results," *15th IMACS World Congress*, Vol. 5, Systems Engineering, Wissenschaft und Technik Verlag, Berlin, 1997, pp. 643–648.

G. M. Faeth
Editor-in-Chief